Paleoceanography and Paleoclimatology journal

Calcareous nannofossils of the late Eocene- early Oligocene from the Pabdeh – Asmari transition in Dezful embayment (SW Iran): Evidence of a climate cooling event

Saeedeh Senemari[1]*, Azam Mahanipour [2]

*[1]Department of Mining, Faculty of Engineering, Imam Khomeini International University, Qazvin, Iran. Tel: +00982833901126-09127852086 (Fax): + 00982833780073 (E- mail):senemari2004@yahoo.com. https://orcid.org /0000-0002-2326-248X

[2] Department of Geology, Faculty of Science, Shahid Bahonar University of Kerman, Kerman, Iran. (E- mail): a_mahanipour@uk.ac.ir. https://orcid.org/0000-0001-6202-6933

key points: paleoclimatology, biostratigraphy, paleoceanography

Contents of this file

Abstract

The Calcareous nannofossil assemblages have been investigated at the uppermost Eocene – lowermost Oligocene at Marun Oil Field in Dezful embayment (SW Iran). The studied interval mainly consists of marly shales, marlstones, and limestones. Seventeen genera and 36 species of calcareous nannofossil have been determined. Regarding the succession of nannofossil bioevents, the studied interval is ranging from late Eocene (Priabonian, CNE18/NP18) to early Oligocene (Rupelian, CNO2/NP22). High relative abundance of warm water taxa (such as *Sphenolithus* spp., *Discoaster* spp. and *Helicosphaera* spp.) is recorded at the late Eocene, while towards the Eocene – Oligocene boundary (EOB), an increase in the relative abundance of cool and temperate taxa (such as *Reticulofenestra* spp., *Cyclicargolithus floridanus*, *Dictyococcites bisecta* and *Markalius inversus*) is identified. A marked decrease in abundance of warm water taxa along with a decrease in species diversity indicate the cooling event at the EOB at Marun Oil Field in Iran similar to other parts of the world.

Key words: Calcareous nannofossils, biostratigraphy, Eocene, Oligocene, paleoecology, Zagros Basin.

1. Introduction

During the middle Eocene (Ca. 37-38 Ma), a warm climate event prevailed, which is characterized as the Middle Eocene Climatic Optimum (MECO) interval (Ozdinova, 2013). Subsequently, a long-term trend of climate cooling is started after the MECO, about 42 million years ago (Villa, 2014) at the late Eocene, before the major climate cooling at the Eocene – Oligocene Boundary (EOB) (Pearson et al., 2008). The expansion of the Antarctic ice sheets to more than 50% is recorded at this time interval with the highest volume at the EOB (Katz et al., 2008; Cramer et al., 2011). Regarding different data, there were some oscillations at the temperature between warming and cooling episodes at this time interval along with a general cooling trend (e.g., Jovane et al., 2007; Zachos et al., 2008). The Eocene-Oligocene cooling event is considered as a global phenomenon (Prothero, 1994; Edgar et al., 2010; Erhardt et al., 2013; Farouk et al., 2013; Villa et al., 2014) that's comparable to the Campanian- Maastrichtian cooling event (Miller et al., 2005). Calcareous nannofossils are very sensitive to temperature. Several studies on the Paleogene strata have confirmed the importance of this group of fossils for paleoclimate and paleoceanographic reconstructions (Persico & Villa, 2004; Villa & Persico, 2006; Villa et al., 2008, 2014). In order to further investigate the EOB, the Eocene – Oligocene interval including the uppermost part of Pabdeh Formation and the lowermost part of Asmari Formation have been investigated based on calcareous nannofossil data at the Marun Oil Field in Zagros belt, Dezful Embayment, SW Iran. These two formations have been investigated from different aspects of paleontology (Mohseni & Al-Aasm, 2004; Behbahani et al., 2010; Sadeghi & Hadavandkhani, 2011; Parvanehnezhad Shirazi et al., 2013; Senemari & Sohrabi Molla Usefi, 2013; Senemari, 2014; Khavari Khorassani et al., 2014; Khavari Khorassani et al., 2015). The main aim of the present study is to use calcareous nannofossil assemblages to determine the exact age of the strata and to determine the location of the EOB at (Pabdeh-Asmari formations) and to determine the response of the calcareous nannofossil assemblages to the late Eocene – early Oligocene climate events in this part of the Zagros Basin in Iran.

2. Geological setting

The Zagros fold-thrust belt is composed of Lurestan Province, Fars Province, and Dezful embayment (Motiei, 1995; Kamali et al., 2006; Lacome et al., 2011). The Zagros belt is a tectonically part of the Alpine – Himalayan orogenic belt and formed with the closure of the Neo-Tethys Ocean after a collision

between the Eurasian and African-Arabian plates (Berberian & Berberian, 1981; Alavi, 2004). The Dezful Embayment is one of the most important regions of the Zagros foreland Basin, that sediments were deposited. Marun Oil Field is one of the biggest oil fields with 67 km long and 7 km wide located in Dezful Embayment, north of the Persian Gulf and southeast of Ahwaz city (Fig. 1). The Pabdeh and Asmari formations are part of the Cenozoic deposits in this oil field (Darvishzadeh, 1992; Alizadeh et al., 2012). In order to investigate the Eocene – Oligocene boundary regarding the calcareous nannofossil assemblages, the upper part of the Pabdeh Formation and the lower part of the Asmari Formation are investigated. The studied interval mainly consists of shale, marlstone, and limestone, located in Marun Oil Field (N 30° 56', E 49° 37'), about 100 km Southeast of Ahwaz city (Fig. 1).

Figure 1. Geological and approximate Geographical location of oilfield, after Beiranvand & Ghasemi-Nejad (2013).

3. Material and Methods

A total of 53 samples from the uppermost part of the Pabdeh Formation and the lower part of the Asmari Formation were analyzed. Samples were processed following a standard smear slide technique (Bown & Young, 1998) that is one of the fastest methods for calcareous nannofossil preparation. All slides were studied under a polarized light microscope at 1000× magnification.

Calcareous nannofossil nomencalture follows the taxonomic scheme of Perch-Nielsen (1985). The NP zonation of Martini (1971) has been applied and a correlation has been done with CNE and CNO zonations of Agnini et al. (2014). For paleoenvironmental analysis, at least 300 specimens were counted in each slide.

4. Results

4. 1. Calcareous nannofossil biostratigraphy

Based on the index calcareous nannofossil bioevents the studied interval is attributed to NP18 to NP22 biozones of Martini (1971) (equivalent with CNE18 to CNO2 biozones of Agnini et al. 2014), which spans from late Eocene (Priabonian) to early Oligocene (Rupelian). The Base (B), Base common (BC), Top (T), and Top common for the most important taxa is illustrated in Fig. 2. Biozones identified in the study section are described below (Plate 1).

4. 1. 1 Isthmolithus recurvus Partial Range Zone (CNE18) (Equivalent of Zone NP18 and the lower undifferentiated Zone NP19/20), lower Priabonian

The base of this biozone was not detected, as top common (TC) *Cribrocentrum erbae* cannot be identified at the studied interval. The top of this biozone was determined by the Base (B) of *Cribrocentrum isabellae* (9 m, sample 12). This biozone was determined from the lowermost part of the studied interval with a thickness of 9 m. Base *Isthmolithus recurvus* was recorded at 5m (sample 7). This biozone is identified at Pabdeh Formation.

4. 1. 2 Cribrocentrum isabellae/Cribrocentrum reticulatum Concurrent Range Zone (CNE19) (Equivalent of the middle part of undifferentiated Zone NP19/NP20), middle Priabonian

This biozone was determined from the Base of *Cribrocentrum isabellae* (9 m, sample 12) to the top of *Cribrocentrum reticulatum* (14 m, sample 18). This biozone is approximately corresponds to the middle part of undifferentiated Zone NP19/NP20. This biozone (NP19) is defined by 5 m thickness at Pabdeh Formation.

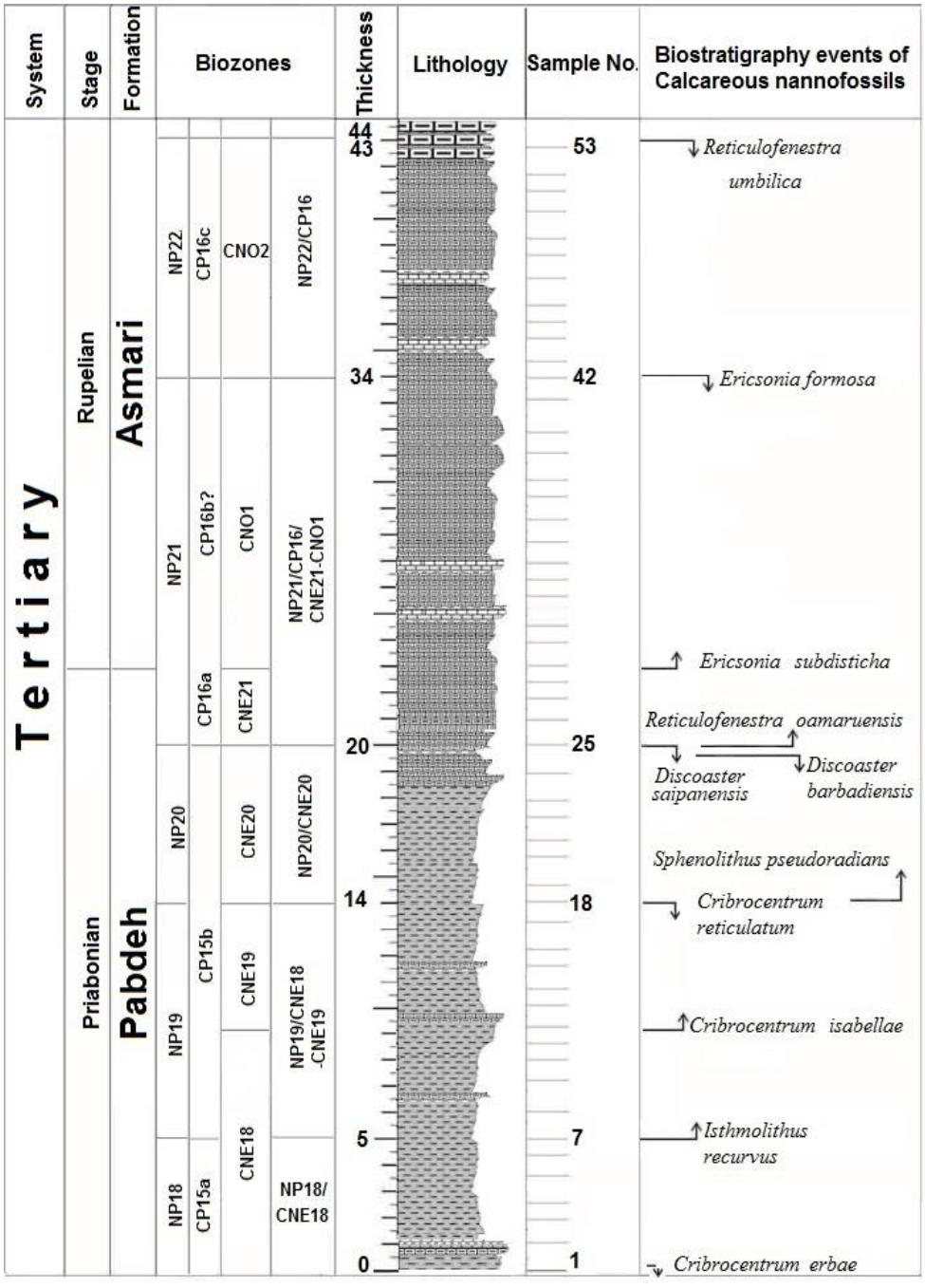

Figure 2. Biostratigraphy of Pabdeh –Asmari Formations interval (EOB).

4. 1. 3 Discoaster Saipanensis Top Zone (CNE20) (Equivalent to the upper part of the undifferentiated Zone NP19/NP20), upper Priabonian

This biozone extends from the Top *Cribrocentrum reticulatum* (14 m, sample 18) to Top *Discoaster saipanensis* (20 m, sample 25). The thickness of this biozone is 6 m at the Pabdeh Formation.

4. 1. 4 Helicosphaera compacta Partial Range Zone (CNE21), (Equivalent to the lower part of Zone NP21), uppermost part of Priabonian

This biozone is defined from the Top of *Discoaster saipanensis* (20 m, sample 25) to Base common (BC) *Clausicoccus subdistichus* (23 m, sample 29), with 3 m thickness at Pabdeh Formation. According to some works from other parts of the world (Backman, 1986; Coccioni et al., 1988; Marino & Flores, 2002; Norris et al., 2014), the high relative abundance of *Clausicoccus subdistichus* was recorded after the Eocene – Oligocene boundary. Regarding these data, BC of *Clausicoccus subdistichus* was considered as a marker for defining the Eocene – Oligocene boundary.

4. 1. 5 Ericsonia formosa/Clausicoccus subdistichus Concurrent Range Zone (CNO1) (Equivalent with the uppermost part of NP21), lowermost part of Rupelian

This biozone extends from BC of *Clausicoccus subdistichus* (23 m, sample 29) to Top *Ericsonia formosa* (34 m, sample 42), with 11 m thickness. This biozone was identified in Asmari Formation.

4. 1. 6 Reticulofenestra umbilicus Top Zone (CNO2) (Equivalent of Zone NP22), lower Rupelian

This biozone extends from the Top of *E. formosa* (34 m, sample 42) to Top *Reticulofenestra umbilicus* (43 m, sample 53). The thickness of this biozone is 9 m and is located at Asmari Formation.

5. Discussion

5. 1. Calcareous nannofossil assemblages

Calcareous nannofossils are sensitive to sea surface temperature, salinity, nutrient, water stratification and depth of the photic zone (Aubry, 1992; Winter & Siesser, 1994; Villa et al., 2008), therefore they can be used as markers for paleoenvironmental reconstructions such as nutrient and temperature.

Quantiative analyses of the late Eocene – early Oligocene show variations in the composition and abundance of the calcareous nannofossils. The most important taxa are *Discoaster* spp. (mean: 21.1%), *Sphenolithus* spp. (mean: 24%), *Ericsonia* subdiscticha (mean: 5.5%), *Dictyococcites bisectus* (mean: 19%), *Cyclicargolithus floridanus* (mean: 25.7%), *Zygrhablithus bijugatus* (mean: 4.6%), *Coccolithus pelagicus* (mean: 12.5%), *Isthmolithus recurvus* (mean: 1.5%), *Reticulofenestra umbilicus* (mean: 6.7%), *Reticulofenestra daviesi* (mean: 7.4%), *Helicosphaera* spp. (mean: 10%).

The paleoecological preferences of the recorded species are considered according to the literatures are as follow:

Discoaster spp. is considered as a warm water taxa that indicates oligotrophic conditions (Bralower, 2002; Kahn & Aubry, 2004; Tremolada & Bralower, 2004; Villa et al., 2008). The highest relative abundance of *Discoaster* is recorded at the middle part of Eocene, while the extinction of the rosette shaped *Discoasters* identified near the Eocene – Oligocene boundary (Miller et al., 2008; Pearson et al., 2008), which might be the result of cooling event (Villa et al., 2008). Although, *Discoasters* can be also affected by the amount of nutrient content of surface waters, but at the EOB the most important factor is low temperature of surface water. At the studied interval, relative abundance of *Discoaster* spp. (*Discoaster deflandrei, Discoaster saipanensis, Discoaster barbadiensis*) is ranging between 1 to 43.6%, while at the EOB the relative abundance of this group is decreasing to zero and again above the boundary at CNO2 biozone, the relative abundance of this group is increasing to 38.9%. *Sphenolithus* spp. is another group of taxa that are regarded as an indicator of oligotrophic and warm water conditions (Aubry, 1998; Bralower,

2002; Gibbs et al., 2004). Some authors (Agnini et al., 2006; Gibbs et al., 2006), believe that nutrient is the most important factor that control the relative abundance of this group. At Marun Oil Field, the relative abundance of this genus is ranging between 0 to 74.5%. The highest relative abundance of this group (*Sphenolithus predistentus, Sphenolithus moriformis, Sphenolithus radians*) is recorded at the late Eocene (74.5%), and a decrease in the relative abundance is recorded towards the EOB and the early Oligocene (3.2% to 18.7%). *Ericsonia* spp. is considered as a warm and oligotroph water taxa (Aubry, 1992; Bralower, 2002; Tremolada & Bralower, 2004). At Marun Oil Filed, *Ericsonia subdisticha* is ranging between 0 to 15.5%. An increase in the relative abundance of *Ericsonia subdisticha* is recorded from the uppermost part of the Eocene to early Oligocene (15.5%). The next important taxa is *Dictyococcites bisectus*, which is considered as a temperate water taxa (e.g., Persico & Villa, 2004). The relative abundance of this genus is fluctuating between 0 to 75%. The highest relative abundance of this species is recorded at early Oligocene interval (75%). Another species is *Cyclicargolithus floridanus* that is regarded as a eutroph species (Aubry, 1992; Monechi et al., 2000), with an affinity to temperate-cold surface water condition (Aubry, 1992). As *C. floridanus* is sensitive to dissolution (Blaj et al., 2009), its high relative abundance at the early Oligocene samples (89.5%) indicates a suitable environment for this species to flourish at the basin.

Zygrhablithus bijugatus is also considered as temperate and eutroph water taxa (Villa et al., 2008) that is mainly recorded at the near shore environments. High relative abundance of this species is recorded at the early Oligocene interval (26.6%). Although *Coccolithus pelagicus* regarded as a warm water taxa at the Paleocene interval but at the Eocene – Oligocene boundary, this species is considered as a temperate-water taxa by Villa et al. (2008). At the studied interval an increase in the relative abundance of this species is recorded at the EOB. (27.5%). Another species that is present at the studied interval is *Isthmolithus recurvus* that is fluctuating between 0 to 5.1%. In some studies, this species is considered as a cool (e.g., Monechi et al., 2000) to temperate

(Persico & Villa, 2004; Villa & Persico, 2006) water taxa. *Reticulofenestra umbilicus* is another taxa that is considered as a temperate water taxa (Persico & Villa, 2004; Villa et al., 2008). High relative abundance of this species is recorded slightly above the EOB (15.5%). *Reticulofenestra daviesi* has an affinity to cool surface water conditions (Persico & Villa, 2004; Villa et al., 2008). High relative abundance of this species (23.7%) is recorded slightly above the EOB at the Oligocene interval of the Marun Oil Field.

Another group of taxa is *Helicosphaera* spp. that is considered as nearshore indicators to prefer either mesotrophic (Young, 1994; Ziveri et al., 2004; Boeckel et al., 2006) or eutroph conditions (Perch-Nielsen, 1985; Wei & Wise, 1990; Giraudeau, 1992). Some authors consider it as warm water taxa (McIntyre & Bé, 1967; Roth & Coulbourn, 1982; Ziveri et al, 2004; Boeckel et al., 2006). The distribution of *Helicosphaera* is complicated by the dissolution-prone nature of the genus also (Perch-Nielsen, 1985). The highest relative abundance of this species is recorded near EOB of the Marun Oil Filed (18.60%).

Regarding these data, *Discoaster* spp. and *Sphenolithus* spp. are considered as warm water taxa, *Reticulufenestra daviesi* as cold water taxa and *Dictyococcites bisecta*, *Cyclicargolithus floridanus*, *Zygrablithus bijugatus*, *Coccolithus pelagicus*, *Isthmolithus recurvus* and *Reticulufenestra umbilicus* as temperate water taxa (Fig. 3). *Discoaster* spp. and *Sphenolithus* spp. are also regarded as oligotroph taxa in contrast to *Cyclicargolithus floridanus*, *Zygrablithus bijugatus*, *Helicosphaera* spp. and *Ericsonia subdisticha* as eutroph taxa. The relative abundance of the mentioned taxa is illustrated at Figures 3, 4, 5 and 6. The highest relative abundance of warm and oligotroph water taxa (e.g., *Discoaster* spp., *Sphenolithus* spp.) can be observed at the late Eocene, while towards the EOB, these warm and oligotroph taxa are decreasing. Simultaneously near the EOB and above the boundary, high relative abundance of eutroph (*Helicosphaera* spp., *C. floridanus, Z. bijugatus, E. subdisticha*) and temperate (e.g., *D. bisectus, C. floridanus, Z. bijugatus, I. recurvus, C. pelagicus, R. umbilicus*) water taxa is recorded. The number of cold water taxa like *R. daviesi*

shows an increasing trend at the E/O boundary and the early Oligocene interval. These abundance patterns and turnovers in nannofossil population are suggesting eutroph and temperate to cool conditions at the E/O boundary and the early Oligocene interval. At the studied interval the relative abundances of temperate and cool water taxa are increasing, while in other locations (Wei et al., 1992; Persico & Villa, 2004; Villa et al., 2008), the relative abundance of temperate water taxa is decreasing along with an increase in the relative abundance of cold water taxa, which might be resulting from the distance with Antarctica.

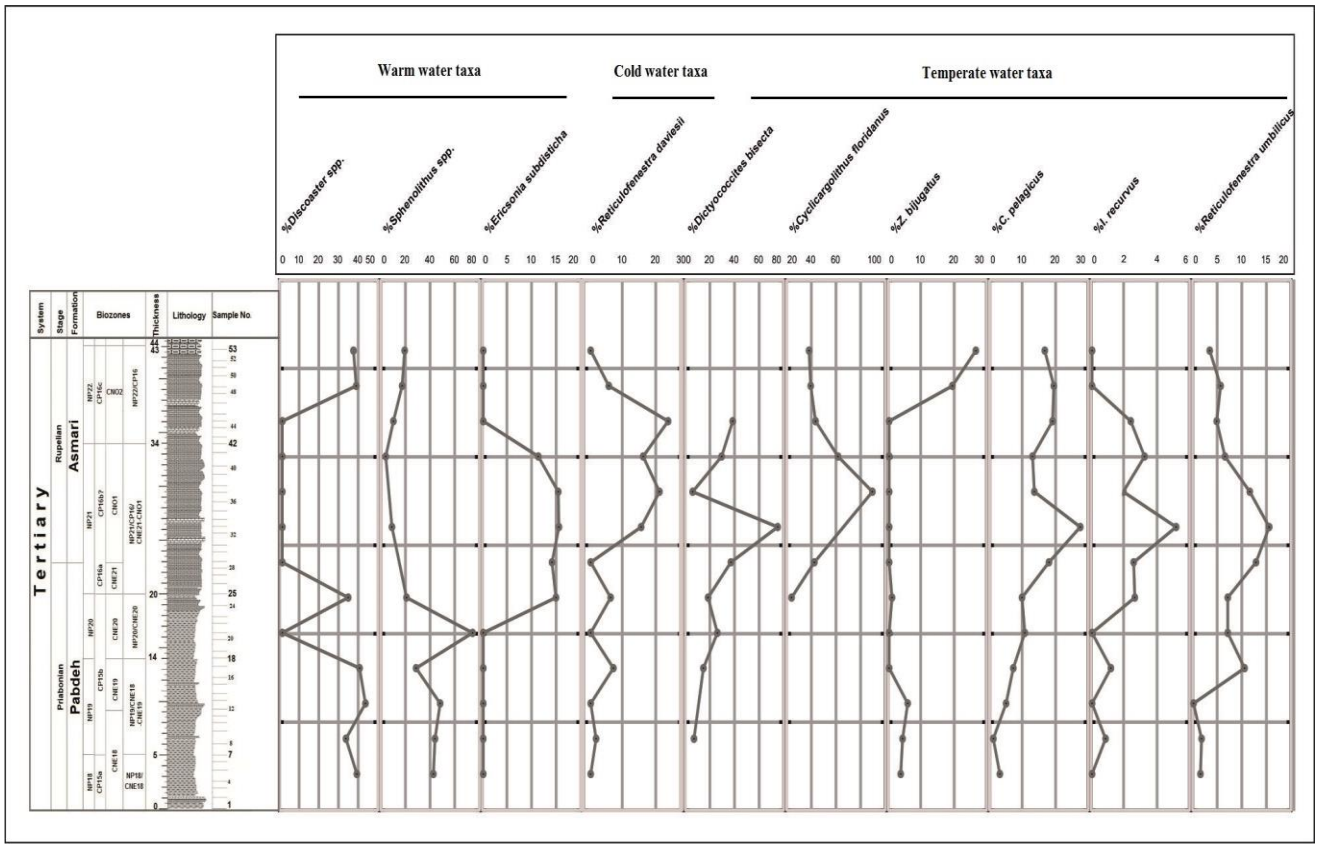

Figure 3. Relative abundance of different water taxa at the upper part of the Pabdeh Formation and lower part of the Asmari Formation (EOB).

Regarding Villa et al. (2008), increase in the relative abundance of *R. daviesi* near the E/O boundary might be the signal for the initiation of the Oligocene Isotope Event 1 (Oi-1 event). A major increase in the relative abundance of this species is recorded at sample 32, which can be considered as a marker for the Oi-1 event (Fig. 3). *Chisamolithus* spp. group which is cold water

taxa, is very rare at the studied interval. Considering Villa et al. (2008), high relative abundance of nutrients at the E/O boundary and the early Oligocene that is recorded from the Kerguelen Plateau has a positive feedback on the cooling event at this time interval. The cooling event at the EOB is also reported from the Southern Ocean (Persico & Villa, 2004) and Southern Indian Ocean (Villa et al., 2008) by focusing on the calcareous nannofossil assemblages and stable isotopes. During this time interval Antarctic glaciations has been recorded by an increase in deep-sea oxygen isotope values at the EOB and the Oligocene time, which are signals for global cooling and/or increasing volume of the ice and are associated with sea level fall (Houben et al., 2012).

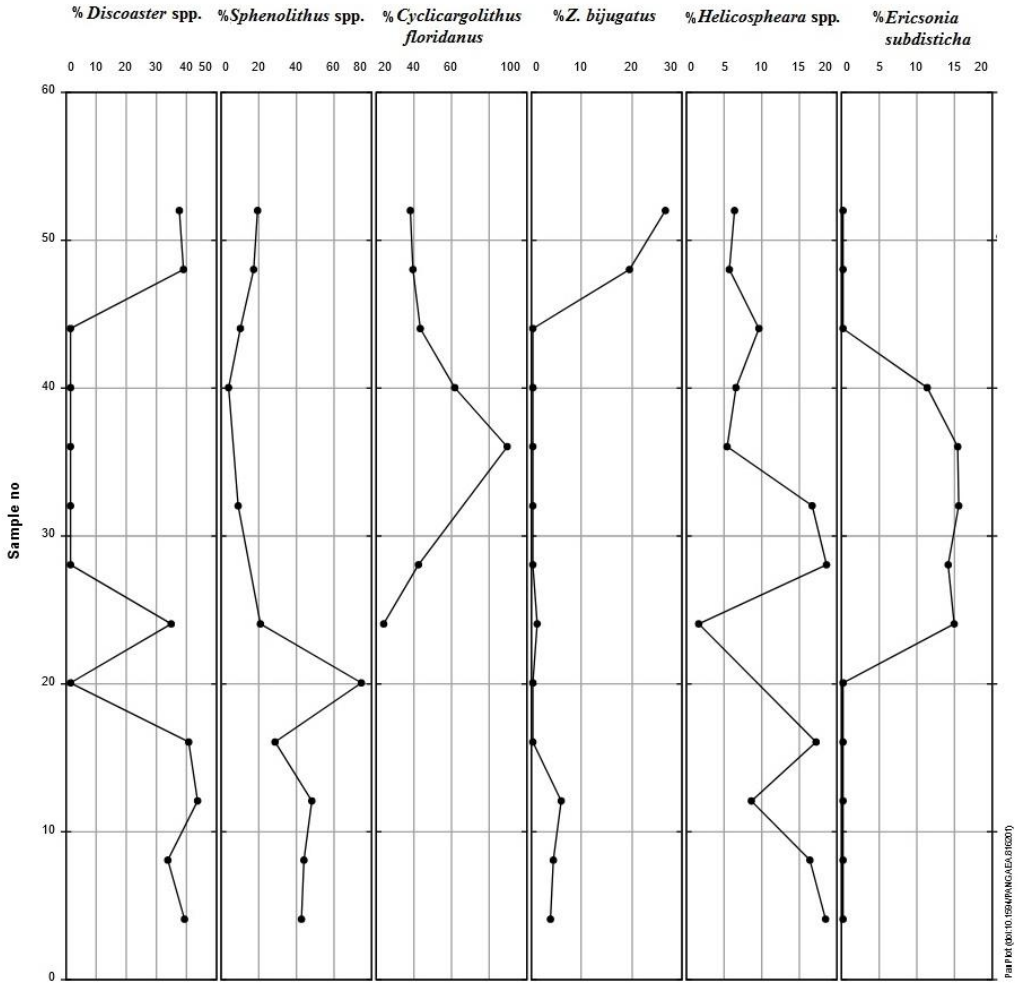

Figure 4. Relative abundance of oligotroph and eutroph taxa at the upper part of the Pabdeh Formation and lower part of the Asmari Formation (EOB).

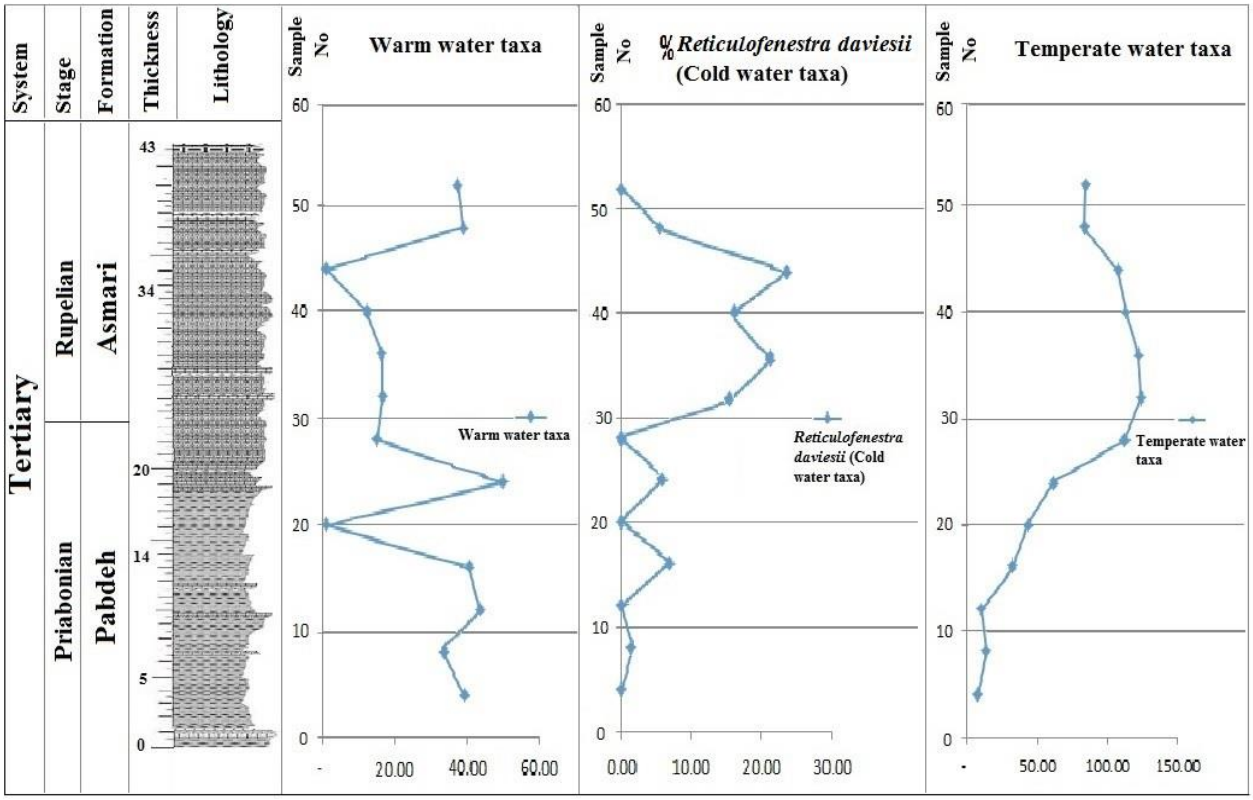

233

234 **Figure 5.** Relative abundance of warm, cold and temperate water taxa at the EOB.

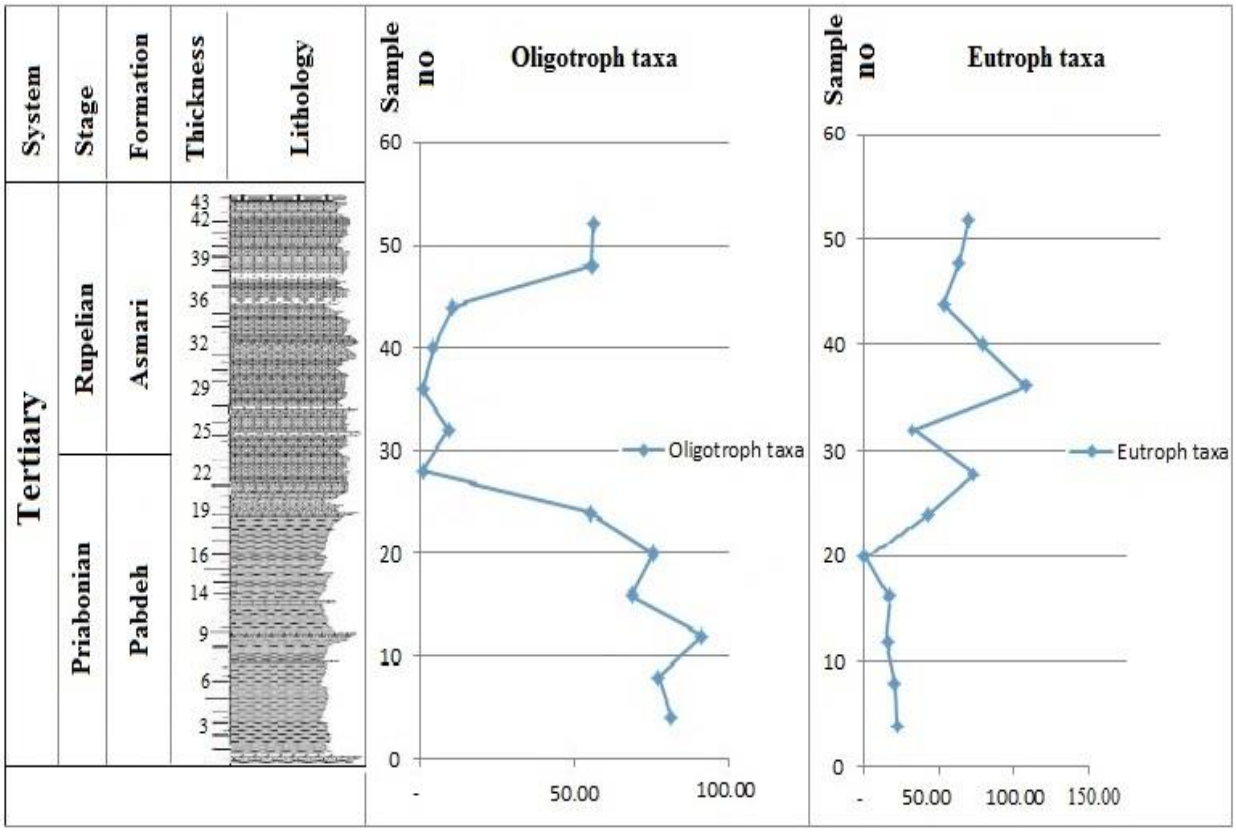

235

236 **Figure6.** Relative abundance of oligotroph and eutroph taxa at the EOB.

237

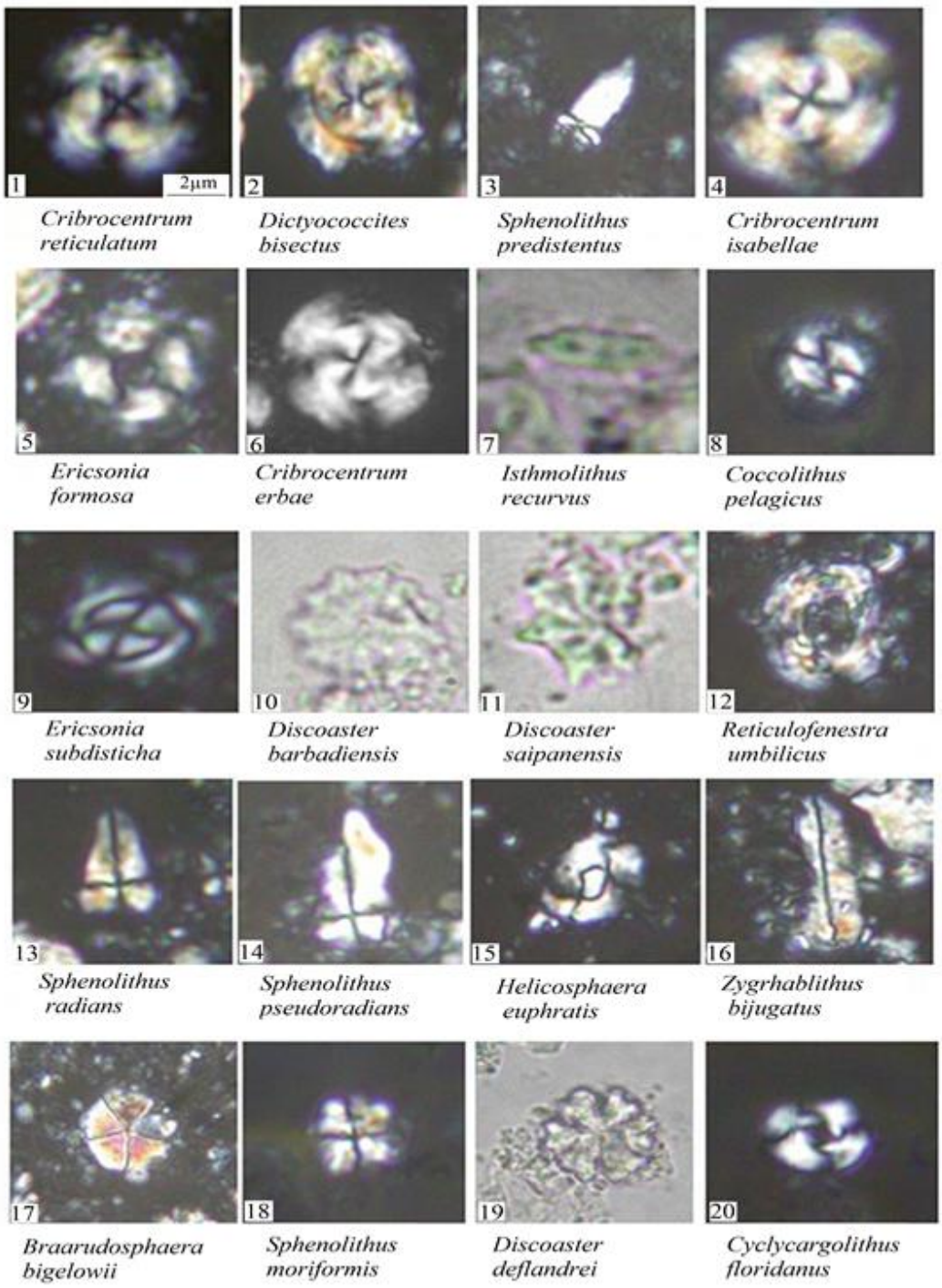

238

239 **Plate 1.** All figures in XPL except figures 7, 10, 11 and 19 in PPL, Light microghraphs1000X; the taxa

240 considered in the present figure are referenced in Perch-Nielsen (1985) and Fornaciari et al. (2010).

241

242 **6. Conclusion**

243 Quantitative analysis of the calcareous nannofossils at Marun Oil field in Dezful embayment (SW

244 Iran) has been used for determining the paleoecological conditions of the uppermost Eocene –

lowermost Oligocene interval. Regarding the calcareous nannofossil data the studied interval is ranging from Priabonian (CNE18/NP18) to Rupelian (CNO2/NP22). High relative abundance of warm water taxa is identified which is replaced by an increase in the relative abundance of temperate and cool taxa in the Eocene – Oligocene boundary (EOB) and above the boundary, which confirms the cooling event at the EOB, similar to other parts of the world.

Acknowledgements

The authors thank all the reviewers for their valuable comments. There is no conflict of interest for authors.

References

Agnini, C., Muttoni, G., Kent, D.V., & Rio, D. (2006). Eocene biostratigraphy and magnetic stratigraphy from Possagno, Italy: the calcareous nannofossil response to climate variability. Earth and Planetary Science Letters 241, 815–830. doi:10.1016/j.epsl.2005.11.005

Agnini, C., Fornaciari, E., Raffi, I., Catanzariti, R., Pälike, H., Backman, J., & Rio, D. (2014). Biozonation and biochronology of Paleogene calcareous nannofossils from low and middle latitudes. *Newsletters on Stratigraphy*, 47(2), 131–181. http://dx.doi: 10.1127/0078-0421/2014/0042

Alavi, M. (2004). Regional Stratigraphy of the Zagros fold-trust belt of Iran and its Proforland evolution. *American Journal Science*, 304, 1–20. http://dx.doi.org/10.2475/ajs.304.1.1

Alizadeh, B., Sarafdokht, H., Rajabi, M., Opera, A. & Janbaz, M. (2012). Organic Geochemistry and petrography of Kazhdumi (Albian-Cenomanian) and Pabdeh (Paleogene) potential source rock in Southern part of the Dezful Embayment, Iran. *Journal of Organic Geochemistry,* 49, 36–46.

Aubry, M.P. (1992). Paleogene Calcareous Nannofossils from the Kerguelen Plateau, Leg 120. In S.W. Wise, & R. Schlich, (Eds.), Proceedings of the Ocean Drilling Program, Scientific Results, Ocean Drilling Program, College Station, pp.471–491.

269 Aubry, M.P. (1998). Early Paleogene calcareous nannoplankton evolution: a tale of climatic
270 amelioration. In M. P., Aubry, S. G., Lucas, W. A. Berggren, (Eds.), Late Paleocene–early Eocene
271 Biotic and Climatic Events in the Marine and Terrestrial Records. Columbia University Press, New
272 York, pp.158–201.
273 Backman, J. (1986). Late Paleocene to middle Eocene calcareous nannofossil biochronology
274 from the Shatsky Rise, Walvis Ridge and Italy, *Palaeogeogr. Palaeocl.*, 57, 43–59.
275 Behbahani, R., Mohseni, H., Khodabakhsh, S. & Atashmard, Z. (2010). Depositional environment
276 of the Pabdeh Formation (Paleogene) elucidated from trace fossils, Zagros Basin, W Iran. 1st
277 International Applied Geological Congress, Iran: 1004-1007.
278 Beiranvand, B. & Ghasemi-Nejad, E. (2013). High resolution planktonic foraminiferal
279 biostratigraphy of the Gurpi Formation, K/PG boundary of the Izeh zone, SW Iran. *Revista*
280 *Brasileira de Paleontologia*, 16(1), 5–26.
281 Berberian, F. & Berberian, M. (1981). Tectonoplutonic episodes in Iran. In Zagros- Hindu Kush-
282 Himalaya Geodynamic Evolution, Washington, D.C. *American Geophysical Union*, 3, 5–32.
283 Blaj, T., Backman, J. & Raffi, I. (2009). Late Eocene to Oligocene preservation history and
284 biochronology of calcareous nannofossils from paleo-equatorial Pacific Ocean sediments. *Rivista*
285 *Italiana di Paleontologia e Stratigrafia*, 115, 67–85.
286 Bown, P.R. & Young, J.R. (1998). Techniques. In P.R. Bown, (Ed.), Calcareous nannofossil
287 Biostratigraphy, Academic Publishers, Dordrecht, Boston, London, pp.16-28.
288 Bralower, T.J. (2002). Evidence of surface water oligotrophy during the Paleocene-Eocene
289 thermal maximum: Nannofossil assemblage data from Ocean Drilling Program Site 690, Maud
290 Rise, Weddell Sea. *Paleoceanography*, 17(2), 1–12.
291 Coccioni, R., Monaco, P., Monechi, S., Nocchi, M., & Parisi, G., (1988). Biostratigraphy of the
292 Eocene–Oligocene bonudary at Massignano (Ancona, Italy). In Premoli Silva, I., Coccioni, R.,

293 Montanari, A. (Eds.), The Eocene– Oligocene Boundary in the March-Umbria Basin (Italy), Fratelli
294 Anniballi. Ancona, pp.81–96.
295 Cramer, B. S., Miller, K. G., Barrett, P. J. & Wright, J. D. (2011). Late Cretaceous – Neogene trends in
296 deep ocean temperature and continental ice volume?: Reconciling records of benthic
297 foraminiferal geochemistry (_18O and Mg=Ca) with sea level history, 116, 1–23,
298 https://doi.org/10.1029/2011JC007255.
299 Darvishzadeh, A. (1992). Geology of Iran. Amirkabir Publication Company, Tehran.
300 Edgar, K.M., Wilson, P.A., Sexton, P.F., Gibbs, S.J., Roberts, A.P. & Norris, R.D. (2010). New
301 biostratigraphic, magnetostratigraphic and isotopic insights into the Middle Eocene Climatic
302 Optimum in low latitudes, *Palaeogeography, Palaeoclimatology, Palaeoecology,* 297, 670–682.
303 Erhardt, A.M., Pälike, H. & Paytan, A. (2013). High-resolution record of export production in the
304 eastern equatorial Pacific across the Eocene- Oligocene transition and relationships to global
305 climatic records, *Paleoceanography*, 28,130–142, doi: 10.1029/2012PA002347
306 Farouk, S., Ahmad, F. & Smadi, A.A. (2013). Stratigraphy of the Middle Eocene–Lower Oligocene
307 successions in north-western and eastern Jordan. *Journal of Asian Earth Sciences*, 73, 396–408.
308 Gibbs, S.J., Shackleton, N.J. & Young, J.R. (2004). Identification of dissolution patterns in
309 nannofossil assemblages: a high-resolution comparison of synchronous records from Ceara Rise,
310 ODP Leg 154. *Paleoceanography*, 19(1), 1029–1041.
311 Gibbs, S.J., Bralower, T.J., Bown, P.R., Zachos, J.C. & Bybell, L.M. (2006). Shelf and open ocean
312 calcareous phytoplankton assemblages across the Paleocene-Eocene thermal maximum:
313 implications for global productivity gradients. *Geology*, 34(3), 233-236.
314 Giraudeau, J., 1992. Distribution of Recent nannofossils beneath the Benguela system:
315 Southwest African continental margin. *Marine Geology*, 108, 219–237.

316 Houben, A.J.P., Mourik, C.V., Montanari, A., Coccioni, R., Brinkhuis, H., (2012). The Eocene–
317 Oligocene transition: Changes in sea level, temperature or both? *Palaeogeography*
318 *Palaeoclimatology Palaeoecology* 335 (2), 75–83.
319 Jovane, L., Sprovieri, M., Florindo, F., Acton, G., Coccioni, R., Dall'Antonia, B., & Dinarès-Turell, J.
320 (2007). Eocene-Oligocene paleoceanographic changes in the stratotype section, Massignano,
321 Italy: Clues from rock magnetism and stable isotopes. *Journal of Geophysical Research*, 112
322 B11101. https://doi.org/10.1029/2007JB004963
323 Kamali, M.R., Fathi Mobarakabad, A. & Mohsenian, E. (2006). Petroleum Geochemistry and
324 Thermal Modeling of Pabdeh Formation in Dezful Embayment. *Journal Science of University*
325 *Tehran*, 32 (2), 1–11.
326 Khavari Khorassani, M., Hadavi, F., Ghasemi-Nejad, E. & Mousavi-Harami, R. (2014).
327 Biostratigraphy and Paleoecological Study of Pabdeh Formation in Interior Fars, Zagros Basin,
328 Iran. *Open Journal of Geology*, 4, 571–581. doi: 10.4236/ojg.2014.411042
329 Khavari Khorassani, M., Ghasemi-Nejad, E., Wagreich, M., Hadavi, F., Richoz, S. & Mousavi Harami,
330 R. (2015). Biostratigraphy and Geochemistry of Upper Paleocene - lower Eocene Oceanic Red
331 Beds from the Zagros Mountains, SW Iran. *Journal Earth Science & Climatic Change*, 6 (8), 302.
332 doi:10.4172/2157-7617.1000302.
333 Kahn, A., & Aubry, M. P. (2004). Provincialism associated with the Paleocene/Eocene thermal
334 maximum: temporal constraint. *Marine Micropaleontology* 52, 117–131. doi:10.
335 1016/j.marmicro.2004.04.003
336 Katz, M. E., K. G. Miller, J. D. Wright, B. S. Wade, J. V. Browning, B. S. Cramer, and Y. Rosenthal
337 (2008). Stepwise transition from the Eocene greenhouse to the Oligocene icehouse. *Nat. Geosci.,*
338 1, 329– 334, doi:10.1038/ ngeo179.
339 Lacome, O., Grasemann, B., & Simpson, G. (2011). Geodynamic Evolution of the Zagros.
340 *Geological Magazine,* 148, 689-691. http://dx.doi.org/10.1017/S0016756811000550.

341 Marino, M., Flores, J. A., (2002). Middle Eocene to Early Oligocene calcareous nannofossil
342 stratigraphy at Leg 177 Site 1090. *Marine Micropaleontology* 45, 383–398.
343 Martini, E. (1971). Standard Tertiary and Quaternary Calcareous Nannoplankton Zonation. In
344 Farniacci, A. (Ed.), Proceedings, 2th International Conference on Planktonic Microfossils, Edizioni
345 Tecnoscienza, Rome, Italy, pp. 739–785.
346 McIntyre and Bé, A.W.H. (1967). Modern Coccolithophoridae of the Atlantic Ocean-I Placoliths
347 and Cyrtoliths. Deep Sea Research 14, 561–597.
348 Miller, K.G., Kominz, M.A., Browning, J.V., Wright, J.D., Mountain, G.S., Katz, M.E., Sugarman, P.J.,
349 Cramer, B.S., Christie-Blick, N. & Pekar, S.F. 2005. The Phanerozoic record of global sea-level
350 change. *Science*, 310, 1293–1298.
351 Miller, K. G., Browning, J. V, Aubry, M. P., Wade, B. S., Katz, M. E., Kulpecz, A. A., & Wright, J. D.
352 (2008). Eocene-Oligocene global climate and sea-level changes: St. Stephens Quarry, Alabama,
353 *B. Geol. Soc. Am.*, 120, 34–53, https://doi.org/10.1130/B26105.1,.
354 Mohseni, H. & Al-Aasm, I.S. (2004). Tempestite deposits on a storm-influenced carbonate ramp:
355 an example from the Pabdeh Formation (Paleogene), Zagros Basin, SW Iran. *Journal of Petroleum*
356 *Geology*, 27(2), 163–178.
357 Monechi, S., Buccianti, A., & Gardin, S., (2000). Biotic signals from nannoflora across the iridium
358 anomaly in the upper Eocene of the Massignano section: evidence from statistical analysis.
359 *Marine Micropaleontology*, 39 (1-4), 219–237.
360 Motiei, H. (1995). Petroleum Geology of Zagros. Geological Survey of Iran, Tehran.
361 Norris, R. D., Wilson, P. A., Blum, P., and the Expedition 342, (2014). Proceedings. IODP, 342:
362 College Station, TX (Integrated Ocean Drilling Program). doi:10.2204/iodp. proc.342.2014
363 Ozdinova, S. (2013). Paleoecological evaluation of calcareous nannofossils from the Eocene and
364 Oligocene sediments of the Subtatric Group of the Western Carpathians. *Mineralia Slovaca*, 45,
365 1–10.

366 Parvanehnezhad Shirazi, M., Bahrami, M., Amiri Bakhtiar, H. & Bamdad, O. (2013). Microfacies,
367 sedimentary environment and paleoecology of Paleocene-Eocene deposits in the Zagros basin,
368 north of Shiraz, southwest Iran. *Historical Biology*, doi: 10.1080/08912963.2013.797970, Publish
369 online.
370 Pearson, P.N., McMillan, I.K., Wade, B.S., Dunkley Jones, T., Coxall, H.K., Bown, P.R. & Lear, C.H.
371 (2008). Extinction and environmental change across the Eocene-Oligocene boundary in
372 Tanzania, *Geology*, 36, 179–182, doi:10.1130/G24308A.1.
373 Perch-Nielsen, K. (1985). Cenozoic Calcareous Nannofossils. In H.M., Bolli, J.B Saunders, & K.
374 Perch-Nielsen, (Eds.), Plankton Stratigraphy, Cambridge University Press, Cambridge, pp.427–
375 554.
376 Persico, D. & Villa, G. (2004). Eocene-Oligocene calcareous nannofossils from Maud Rise and
377 Kerguelen Plateau (Antarctica): Paleoecological and paleoceanographic implications. *Mar.*
378 *Micropaleontol.*, 52, 153–179, https://doi.org/10.1016/j.marmicro.2004.05.002.
379 Prothero, D.R. (1994). The late Eocene-Oligocene extinctions. *Annu. Rev. Earth Planet. Sci.*, 22,145-
380 165.
381 Roth, P. H., & Coulbourn, W. T, (1982). Floral and solution pattern of coccoliths in surface
382 sediments of the North Pacific. *Mar. Micropaleontol,* 7, 1–52.
383 Sadeghi, A. & Hadavandkhani, N. (2011). Biostratigraphy of Pabdeh Formation in Emamzadeh
384 Soltan Ebrahim section, Northwest of Izeh city in Khuzestan Province, southern Iran. *Iranian*
385 *Journal of Geology,* 15, 81–98.
386 Senemari, S. & Sohrabi Molla Usefi, M. (2013). Evaluation of Cretaceous–Paleogene boundary
387 based on calcareous nannofossils in section of Pol Dokhtar, Lorestan, southwestern Iran. *Arabian*
388 *Journal of Geosciences*, 6, 3615–3621.
389 Senemari, S. (2014). Diversity changes among calcareous nannofossil assemblages across the
390 Paleocene/Eocene Boundary in the Zagros (Southwest Iran). *Journal of Tethys*, 2, 45–54.

391 Tremolada, F., & Bralower, T. J., (2004). Nannofossil assemblage fluctuations during the
392 Paleocene – Eocene Thermal Maximum at Sites 213 (Indian Ocean) and 401 (North Atlantic
393 Ocean): palaeoceanographic implications. *Marine Micropaleontology* 52, 107–116.
394 doi:10.1016/j.marmicro.2004. 04.002
395 Villa, G., Fioroni, C., Persico, D., Roberts, A.P. & Florindo, F. (2014). Middle Eocene to Late
396 Oligocene Antarctic glaciation/ deglaciation and Southern Ocean productivity.
397 *Paleoceanography*, 29, 223–237, doi: 10.1002/ 2013PA002518
398 Villa G. & Persico D. (2006). Late Oligocene climatic changes: Evidence from calcareous
399 nannofossils at Kerguelen Plateau Site 748 (Southern Ocean). *Palaeogeography,*
400 *Palaeoclimatology, Palaeoecology*, 231, 110–119.
401 Villa G. Fioroni C. Pea L. Bohaty S.M. & Persico D. (2008). Middle Eocene–late Oligocene climate
402 variability: Calcareous nannofossil response at Kerguelen plateau, Site 748. *Marine*
403 *Micropaleontology*, 69, 173–192.
404 Wei, W., & S. W. Wise (1990), Biogeographic gradients of middle Eocene-Oligocene calcareous
405 nannoplankton in the South Atlantic Ocean. *Palaeogeogr. Palaeoclimatol. Palaeoecol.,* 79, 29 – 61,
406 doi:10.1016/0031- 0182(90)90104-F.
407 Wei, W., G. Villa, & S. W. Wise (1992), Paleoceanographic implications of Eocene- Oligocene
408 calcareous nannofossils from Sites 711 and 748 in the Indian Ocean. *Proc. Ocean Drill. Program*
409 *Sci. Results*, 120, 979– 999.
410 Winter, A.,& Siesser, W. G. (Eds) (1994). *Coccoithophores.* Cambridge University Press, Cambridge,
411 242 pp.
412 Young, J.R., (1994). The functions of coccoliths. In A., Winter, W.G. Siesser, (Eds.),
413 Coccolithophores. Cambridge University Press, London, pp. 63–82.
414 Zachos, J. C., Dickens, G. R., & Zeebe, R. E. (2008). An early Cenozoic perspective on greenhouse
415 warming and carbon-cycle dynamics. *Nature*, 451, 279–283, doi:10.1038/nature06588,.

Ziveri, P., Baumann, K.-H., Boeckel, B., Bollmann, J., Young, J., (2004). Biogeography of selected Holocene coccoliths in the Atlantic Ocean. In H.R., Thierstein, J.R. Young, (Eds.), Coccolithophores from Molecular Processes to Global Impact. Springer, Berlin, pp. 400–452.

Captions Figures and Plate

Fig. 1 Geological and approximate Geographical location of oilfield, after Beiranvand and Ghasemi-Nejad (2013).

Fig. 2 Biostratigraphy of Pabdeh –Asmari Formations interval (EOB).

Fig. 3 Relative abundance of different water taxa at the upper part of the Pabdeh Formation and lower part of the Asmari Formation (EOB).

Fig. 4 Relative abundance of oligotroph and eutroph taxa at the upper part of the Pabdeh Formation and lower part of the Asmari Formation (EOB).

Fig. 5 Relative abundance of warm, cold and temperate water taxa at the EOB.

Fig. 6 Relative abundance of oligotroph and eutroph taxa at the EOB.

Plate. All figures in XPL except figures 7, 10, 11 and 19 in PPL, Light microghraphs1000X; the taxa considered in the present figure are referenced in Perch-Nielsen (1985) and Fornaciari et al. (2010).